Carbochlorination of Tantalum and Niobium Oxides: Thermodynamic Simulation and Kinetic Modeling

Fenglin Yang and Vladimir Hlavacek
Laboratory for Ceramic and Reaction Engineering, Dept. of Chemical Engineering,
State University of New York at Buffalo, Amherst, NY 14260

Carbochlorination reactions of tantalum and niobium pentoxides represent an interesting route of extraction of tantalum and niobium from ores or minerals. Both reactions have not been systematically studied in the literature. The kinetic study reported here was carried out in a fixed-bed reactor in a temperature domain $T = 800-1{,}000°C$. The products of the reaction under the conditions studied are in the gaseous phase. With CO as a reducing agent, the reactions in question are of the noncatalytic gas−solid type, and the experimental data fit the shrinking core model. When using carbon as a reducing agent, the reactions are of the gas−solid−solid type, and the reactivity is much higher than that using CO alone. A reaction model based on phase boundary control was used to process the experimental data. Thermodynamic calculations revealed that at temperatures below 1,000°C the carbochlorination reactions result in the corresponding pentachlorides.

Introduction

Tantalum and niobium metals possess several unique physical properties, which render them important for certain special applications. Tantalum is used as an electrolytic capacitor. Tantalum-based alloys feature very high resistance to hot mineral acids, and therefore they are used for the construction of chemical equipment as heat exchangers, pipes, and valves. In superalloys tantalum contributes mainly to such properties as high-temperature strength, reduction in fatigue at high temperatures, and reduction of corrosion by sea air. Niobium has good resistance toward corrosive chemicals, even at high temperatures, and is therefore also used in the construction of chemical equipment. Niobium exhibits a low neutron capture cross section and is highly resistant to corrosion by liquid sodium, and is therefore used in the industry for the production of cans for fuel elements. Niobium-zirconium alloy is used for the sealing caps of sodium vapor lamps.

The minerals that supply practically all of the world's demand for tantalum and niobium are are tantalite, columbite, and pyrochlore. The minerals range in composition between high-grade tantalite containing about 84% Ta_2O_5 to high-grade columbite with about 77%Nb_2O_5 (Johnstone and Johnstone, 1961). Pyrochlore, which contains 40–65% of niobium oxide, is the most important niobium-containing mineral. Owing to the very refractory character of minerals containing tantalum and niobium and the increasing demand for both metals in a high degree of purity, many investigations (Miller, 1959) tried to replace the long and tedious traditional processes by a more straightforward procedure. The classic extraction process is based on fusing the ore concentrate with caustic soda, followed by water extraction, acid treatments, and fractional crystallization of the tantalum or niobium salts.

The chlorination process described in this article is an effective way of extracting tantalum and niobium. It provides a good yield in metal recovery at a reasonable cost (Yang and Hlavacek, 1997, 1998). In this process, the solid metal oxide reacts with a gaseous chlorinating agent in the presence of a reductant such as C or CO, to form metal chlorides. The chlorides are volatile at the operating temperatures. They are carried away by the gas stream, condensed, and then separated by rectification to yield high-purity products. The pure chlorides can be further processed to get pure metals.

The processes of high-temperature chlorination of ores or concentrates rich in niobium and/or tantalum have attracted attention since 1950s. However, quantitative data on the kinetics are not available in the literature. Recently, Freitas and Ajersch (1984) published a report describing the kinetics of chlorination of large granules of niobium oxide by a gaseous

Correspondence concerning this article should be addressed to F. Yang.

mixture of Cl_2/CO. The authors of this article claimed that $NbOCl_3$ was the major metal chloride generated at temperatures ranging from 773 K to 1973 K.

Since tantalum and niobium in the ores are primarily in the form of oxides, a systematic study of the chlorination reactions of their pure oxides is very important for understanding the complex phenomena of the chlorination process. Consequently, our work described below was focused on the kinetic and thermodynamic study of the carbochlorination reactions of Ta_2O_5 and Nb_2O_5 in the high-temperature domain.

Reactor System and Experimental Procedure

Reactor system

The reactor consisted of a quartz tube (OD 32.5 mm, wall thickness 2.5 mm, and length 760 mm), which was placed in a Lindberg tube furnace (1,100°C, TF 55030 A) that was equipped with a temperature controller. The solid sample in powder form was held in a ceramic boat (length 70 mm, width 14 mm, and depth 10 mm) located inside the reactor tube. Gaseous reactants stored in the cylinders were introduced to the inlet of the reactor through plastic tubing. Mass flowmeters and metering valves were used to control the flow rate. Two-stage scrubbers with 5% caustic soda solution neutralized the exit gas.

The temperature inside the reactor tube was determined indirectly through calibration by measuring the local axial temperature profile inside the tube under a blank run, that is, with an inert gas.

Supporting equipment

An analytical balance (Model 200, Sartorius Corporation, Long Island, NY) was used for the measurement of the sample mass before and after chlorination. The balance has a maximum sensitivity of 0.0001 g. The mixing of oxide and carbon powder was accomplished by using a Turbula Shaker-Mixer (Type T2C, Impandex Inc., Haywood, NJ). A thermogravimetric analyzer (TGA) (Model ST-736—temperature ranging from 20°C to 1,600°C and a maximum sensitivity of 0.0001 g—Harrop Industries, Columbus, OH) was used to determine the contents of unreacted oxide and carbon in the chlorinated sample. The particle size of the reacting sample was characterized by the measurement of the BET surface area (Model ASAP2000, Micromeritics Instrument Corporation, Norcross, GA).

Procedure

The samples chlorinated were either pure oxides, Ta_2O_5 (99% metal basis, −325 mesh) or Nb_2O_5 (99.5% metal basis, −100 mesh), or oxides premixed with carbon powder (carbon black MN1100, 14 nm). Argon was selected as a gas for purging before and after chlorination.

The ceramic boat containing a known amount of the sample (0.55 g for pure oxides and 0.80 g for oxide/carbon mixtures) was slowly inserted in the middle of the reactor, the reactor was sealed, and argon was introduced at a flow rate of 200 mL/min to purge the system. The reaction temperature (either 800°C or 1,000°C) was set and the furnace was switched on. The heating rate was 80°C/min. Ten minutes after the temperature reached the set point, the argon flow was shut off and gaseous reactants (Cl_2 or $CO/Cl_2 = 1.7$) were fed into the reactor at the desired flow rate. After the specified chlorination time elapsed, the Cl_2 or Cl_2/CO gas was replaced by argon to purge the system. The reaction temperature was kept for five more minutes in the argon stream to ensure complete removal of the volatile chlorides produced. Afterwards, power was switched off and the furnace body was opened for a quick cooling. After the reactor tube was cooled to room temperature, the purging gas was switched off and the sample was taken out and weighed. For samples of oxide mixed with carbon, TGA analysis was conducted to determine the conversion of oxides.

Thermodynamic Simulation

Thermodynamic simulations of the $Ta_2O_5/Cl_2/CO$, $Nb_2O_5/Cl_2/CO$, $Ta_2O_5/Cl_2/C$, and $Nb_2O_5/Cl_2/C$ reaction systems were performed by using the recent version of NASA Lewis Research Center's computer program for calculating complex equilibria (McBride and Gorden, 1996). This program is based on the minimization of free energy.

For the preceding reaction systems, the initial amount of the reactants was $Ta_2O_5(s) = 1$ mol, $Cl_2 = 15$ mol, $CO = 25.5$ mol; $Nb_2O_5(s) = 1$ mol, $Cl_2 = 15$ mol, $CO = 25.5$ mol, $Ta_2O_5(s) = 1$ mol, $Cl_2 = 10$ mol, $C(s) = 8$ mol; and $Nb_2O_5(s) = 1$ mol, $Cl_2 = 10$ mol, $C(s) = 8$ mol. The initial compositions resemble the real reaction systems in which a sufficient amount of gaseous reactant(s) flow(s) through the bed of solid reactants. Chemical equilibrium compositions of these reaction systems at different reaction temperatures and normal pressure were obtained and plotted in Figures 1 to 4.

From the results reported in Figures 1 to 4, the following conclusions can be drawn for the chlorination of Ta_2O_5 and Nb_2O_5 with either CO or C as reductant:

1. Ta_2O_5 and Nb_2O_5 have almost identical equilibrium conversion.

2. Ta_2O_5 or Nb_2O_5 can be converted to completion at all temperatures considered (200−1,200°C).

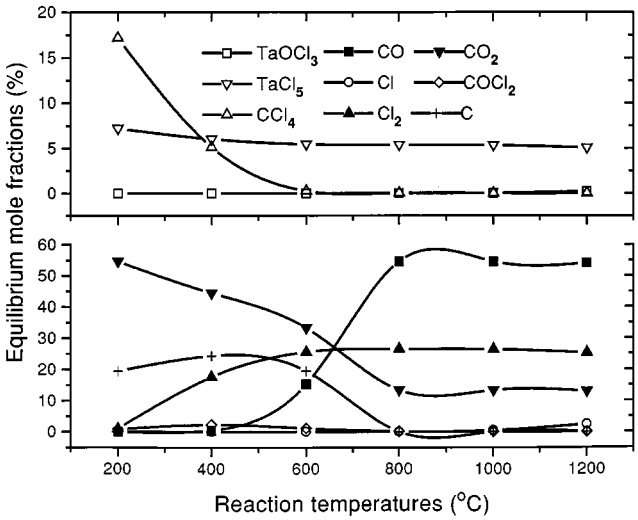

Figure 1. Chemical equilibrium compositions for reactants: $Ta_2O_5(s) = 1$ mol; $Cl_2 = 15$ mol; $CO = 25.5$ mol.

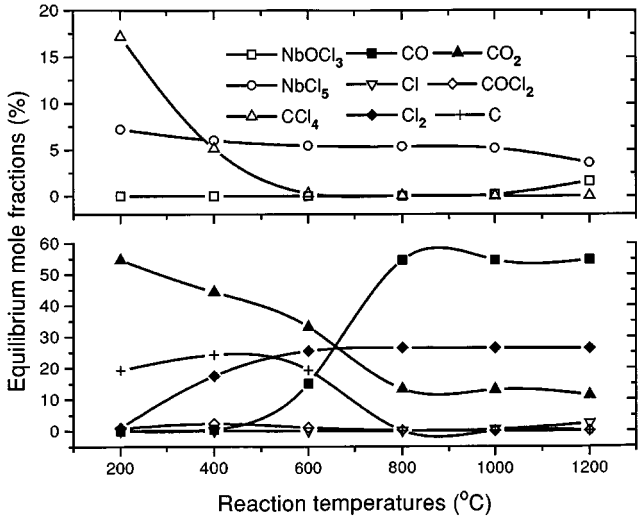

Figure 2. Chemical equilibrium compositions for reactants: $Nb_2O_5(s) = 1$ mol; $Cl_2 = 15$ mol; CO = 25.5 mol.

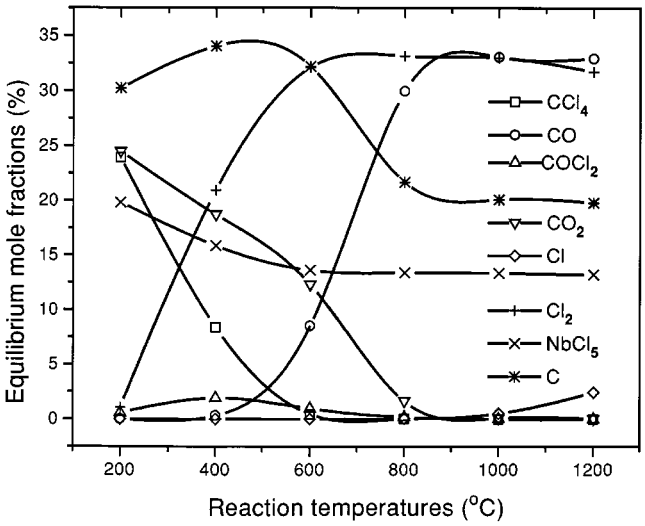

Figure 4. Chemical equilibrium compositions for reactants: $Nb_2O_5(s) = 1$ mol; $Cl_2 = 10$ mol; C = 8 mol.

3. $TaCl_5$ and $NbCl_5$ are the most important products of the chlorination process in the temperature range considered.

4. CCl_4 is produced only when the temperature is below 600°C.

5. $COCl_2$ concentration is always low at all temperatures considered. The Cl· radical was only at observed at temperatures higher than 1,000°C.

Another observation is that for $Ta_2O_5/Cl_2/C$ and $Nb_2O_5/Cl_2/C$ reaction systems, low temperature favors the formation of CO_2; at temperatures higher than 800°C CO becomes dominant.

With CO as a reductant, the important reactions are listed below; here M represents either Ta or Nb:

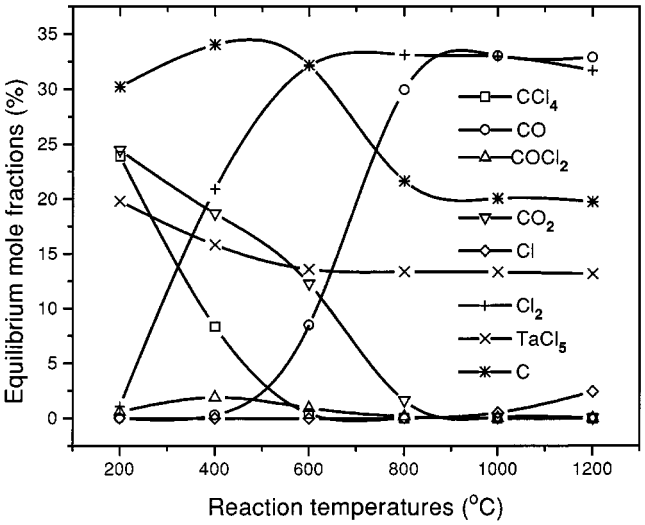

Figure 3. Chemical equilibrium compositions for reactants: $Ta_2O_5(s) = 1$ mol; $Cl_2 = 10$ mol; C = 8 mol.

$$M_2O_5 + 5CO + 5Cl_2 \rightarrow 2MCl_5 + 5CO_2 \quad (1)$$

$$M_2O_5 + 3CO + 3Cl_2 \rightarrow 2MOCl_3 + 3CO_2. \quad (2)$$

Based on the analysis just presented, the most important reaction occurring at temperatures $T = 800$ to 1,000°C is represented by Eq. 1. Therefore, in our kinetic analysis we assume that the MCl_5 is the only chloride generated and M_2O_5 is the only solid phase in this temperature range.

When C is used as a reductant, the following reactions may occur:

$$M_2O_5 + 5C + 5Cl_2 \rightarrow 2MCl_5 + 5CO \quad (3)$$

$$2M_2O_5 + 5C + 20Cl_2 \rightarrow 4MCl_5 + 5CO_2 \quad (4)$$

$$M_2O_5 + 5CO + 5Cl_2 \rightarrow 2MCl_5 + 5CO_2. \quad (5)$$

However, in the temperature range $T = 800$–1,000°C, Eq. 3 is the reaction that plays a dominant role.

Other possible reactions in the reaction systems are insignificant, especially in the temperature range of 800–1,000°C:

$$CO + Cl_2 \rightarrow COCl_2 \quad (6)$$

$$C + 2Cl_2 \rightarrow CCl_4 \quad (7)$$

$$Cl_2 \rightarrow 2Cl \quad (8)$$

$$C + CO_2 \leftrightarrow 2CO. \quad (9)$$

Kinetic Modeling and Experimental Data Fitting

In the quantitative description presented below we continue to use M to represent Ta or Nb.

$Ta_2O_5/Cl_2/CO$ and $Nb_2O_5/Cl_2/CO$ reaction systems

Reaction model. As was discussed earlier, the system is a "gas–solid" type at temperatures $T = 800$–1,000°C and at-

mospheric pressure. MCl_5 is the product considered. The solid M_2O_5 particle is considered to be nonporous. The reaction is of the type:

$$M_2O_5(s) + 5Cl_2(g) + 5CO(g) \rightarrow 2MCl_5(g) + 5CO_2(g). \quad (10)$$

The reaction products are in the gaseous state and no ash is formed on the surface of the solid particle during the reaction; the reacting particle shrinks as the reaction proceeds, and finally disappears.

The reaction mechanism can be described by the following three consecutive steps (Levenspiel, 1972):

Step 1. Diffusion of gaseous reactants, Cl_2 and CO, from the bulk of the gas stream through the gas film to the surface of the M_2O_5 solid particle. It should be emphasized that the particle is nonporous.

Step 2. Surface reaction of gaseous reactants, Cl_2 and CO, with the solid M_2O_5 particle.

Step 3. Diffusion of reaction products, MCl_5 and CO_2, from the surface of the solid through the gas film back into the bulk of the gas stream.

To determine the intrinsic kinetics, the reaction conditions were chosen such that the mass-transfer steps (steps 1 and 3) did not control the overall reaction rate. In the experiments we must work with a sufficiently small sample size and a high gas flow rate. The sample size we used (0.55 g) was small enough to guarantee a low bed depth while being sufficiently large to keep the mass change measurement error under control.

The value of the flow rate necessary to eliminate the mass-transfer resistance was obtained experimentally. The following reaction conditions were selected: $t = 5$ min, $T =$ 1,000°C, $P_{\text{total}} = 102.1$ kPa, $p_{Cl_2} = 37.6$ kPa, and $p_{CO} = 64.5$Pa. The experimental results indicated that the conversion increased with gas flow rate; for gas flow rates higher than 500 mL/min, the conversion remained constant. Therefore, our kinetic experiments were performed with a flow rate of 500 mL/min, with a ratio of $CO/Cl_2 = 1.7$.

Because the mass-transfer steps (steps 1 and 3) were eliminated, the surface chemical reaction rate became the only rate-limiting step (step 2). In this particular case, the model of ''shrinking unreacted solid particle'' with the surface chemical reaction as the rate-controlling step describes the reaction system.

Let us assume that the reaction is irreversible and that the M_2O_5 particle has spherical geometry. Based on the unit surface of the shrinking particle, the rate of the reaction:

$$M_2O_5(s) + 5Cl_2(g) + 5CO(g) = 2MCl_5(g) + 5CO_2(g) \quad (11)$$

can be expressed as follows (Levenspiel, 1972):

$$-\frac{1}{4\pi r^2}\frac{dN_{M_2O_5}}{dt} = -\frac{1}{5\times 4\pi r^2}\frac{dN_{Cl_2}}{dt} = -\frac{1}{5\times 4\pi r^2}\frac{dN_{CO}}{dt} = k_s p_{Cl_2}^m p_{CO}^n. \quad (12)$$

Here, k_s is the rate constant for the surface reaction.

Writing $N_{M_2O_5}$ in terms of the shrinking radius, we have

$$-dN_{M_2O_5} = -d(\rho_{M_2O_5}V) = -\rho_{M_2O_5}dV = -\rho_{M_2O_5}d\left(\frac{4}{3}\pi r^3\right) = -4\pi\rho_{M_2O_5}r^2dr. \quad (13)$$

After substitution of Eq. 13 in Eq. 12 the reaction rate can be expressed in terms of the shrinking radius of the unreacted core,

$$-\rho_{M_2O_5}\frac{dr}{dt} = k_s p_{Cl_2}^m p_{CO}^n. \quad (14)$$

After integration of Eq. 14, we have

$$-\rho_{M_2O_5}\int_{r_o}^{r} dr = k_s p_{Cl_2}^m p_{CO}^n \int_0^t dt \quad (15)$$

$$t = \frac{\rho_{M_2O_5}}{k_s p_{Cl_2}^m p_{CO}^n}(r_0 - r). \quad (16)$$

The time τ necessary for the complete conversion of the particle can be calculated when $r = 0$, that is,

$$\tau = \frac{\rho_{M_2O_5} r_o}{k_s p_{Cl_2}^m p_{CO}^n}. \quad (17)$$

Combining Eqs. 16 and 17 and also noting that

$$1 - X_{M_2O_5} = \frac{V_{\text{unreacted}}}{V_{\text{total}}} = \frac{\frac{4}{3}\pi r^3}{\frac{4}{3}\pi r_o^3} = \left(\frac{r}{r_o}\right)^3,$$

we can get the following relation between reaction time and the shrinking radius (or conversion of the particle) in terms of τ:

$$\frac{t}{\tau} = 1 - \frac{r}{r_o} = 1 - \left(1 - X_{M_2O_5}\right)^{1/3}. \quad (18)$$

Fitting of Experimental Data. Equation 18 can be expressed in the following form:

$$\left(1 - X_{M_2O_5}\right)^{1/3} = 1 - \frac{t}{\tau}. \quad (19)$$

Clearly, the plot of $(1 - X_{M_2O_5})^{1/3}$ vs. t should yield a straight line with a slope of $-1/\tau$.

The ''conversion vs. time relation'' was obtained experimentally at 800°C and 1,000°C, with flow rate = 500 mL/min, $P_{\text{total}} = 102.1$ kPa, $p_{Cl_2} = 37.6$ kPa, and $p_{CO} = 64.5$ kPa. The plots discussed are shown in Figures 5 and 6. The slopes and the corresponding values of τ are:

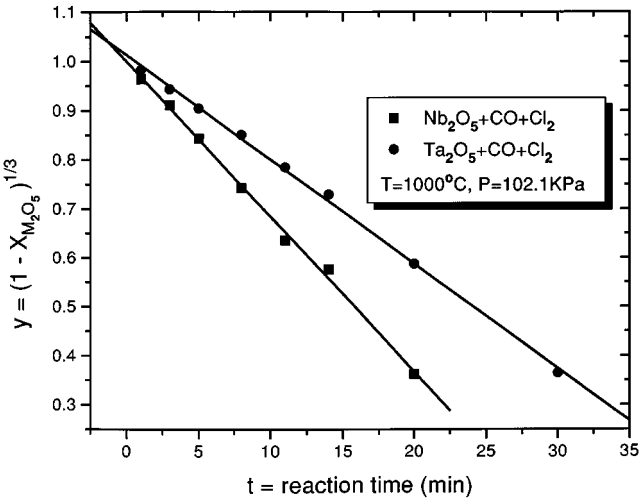

Figure 5. Conversion of M_2O_5 vs. time at 1,000°C.

For Ta_2O_5:

at 1,000°C: $-\dfrac{1}{\tau_{1,000^\circ C}} = -0.02129$ $\tau_{1,000^\circ C} = 46.97$ min

at 800°C: $-\dfrac{1}{\tau_{800^\circ C}} = -0.00776$ $\tau_{800^\circ C} = 128.87$ min.

For Nb_2O_5:

at 1,000°C: $-\dfrac{1}{\tau_{1,000^\circ C}} = -0.03162$ $\tau_{1,000^\circ C} = 31.63$ min

at 800°C: $-\dfrac{1}{\tau_{800^\circ C}} = -0.00615$ $\tau_{800^\circ C} = 162.60$ min.

The value of the rate constant, k_s, can be calculated from Eq. 17, provided that the values of reaction order and other physical properties such as the particle size and density of the solids are available.

Determination of Reaction Order. The reaction rate expression is considered in the following form:

$$r = k_s p_{Cl_2}^m p_{CO}^n. \tag{20}$$

To determine the reaction order, experiments were conducted in the following two stages.

Stage One: Determination of m. The reaction was carried out at constant P_{total} (= 102.1 kPa) and p_{CO} (= 23.8 kPa) pressures. The conversion of M_2O_5 at a different p_{Cl_2} was measured. The following reaction conditions were investigated: temperature = 1,000°C, flow rate = 500 mL/min, reaction time = 2 min. Argon was used as the dilution gas to keep the values of flow rate, P_{total}, and p_{CO} constant while changing the value of p_{Cl_2}. Under these conditions, Eq. 20 can be written in the form:

$$r = k'_s p_{Cl_2}^m. \tag{21}$$

Here

$$k'_s = k_s p_{CO}^n.$$

The experimental data shown in Figure 7 indicate that the plots of "p_{Cl_2} vs. conversion rate" ($\Delta X_{Ta_2O_5}/\Delta t$, and $\Delta X_{Nb_2O_5}/\Delta t$) are represented by straight lines. Evidently, the reaction is first order with respect to Cl_2, that is, $m = 1$, for both Ta_2O_5 and Nb_2O_5.

Stage Two: Determination of n. The reaction conditions were similar to those described in stage one; the only difference was that $p_{Cl_2} = 23.8$ kPa remained constant.

The logarithmic form of Eq. 20 is

$$\ln r = n \ln p_{CO} + \ln\left(k_s p_{Cl_2}\right). \tag{22}$$

The plots of "ln p_{CO} vs. ln($\Delta X_{Ta_2O_5}/\Delta t$) and ln($\Delta X_{Nb_2O_5}/\Delta t$)," recorded in Figure 8, create straight lines. The slopes measured are $n = 0.902$ for Ta_2O_5 and $n = 0.770$ for Nb_2O_5.

Particle Size and Density of Solid Oxides.. The densities $\rho_{Ta_2O_5}^{mass} = 8.20$ g/cm^3 and $\rho_{Nb_2O_5}^{mass} = 4.47$ g/cm^3 were provided by the manufacturer, and the corresponding molar densities are $\rho_{Ta_2O_5} = 0.0186$ mol/cm^3 and $\rho_{Nb_2O_5} = 0.0168$ mol/cm^3.

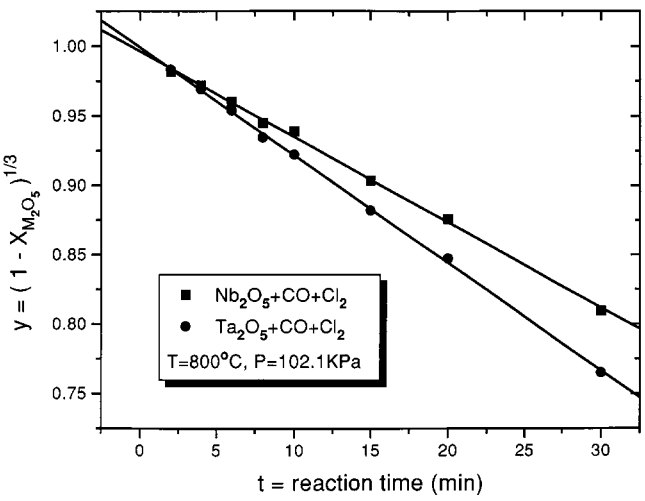

Figure 6. Conversion of M_2O_5 vs. time at 800°C.

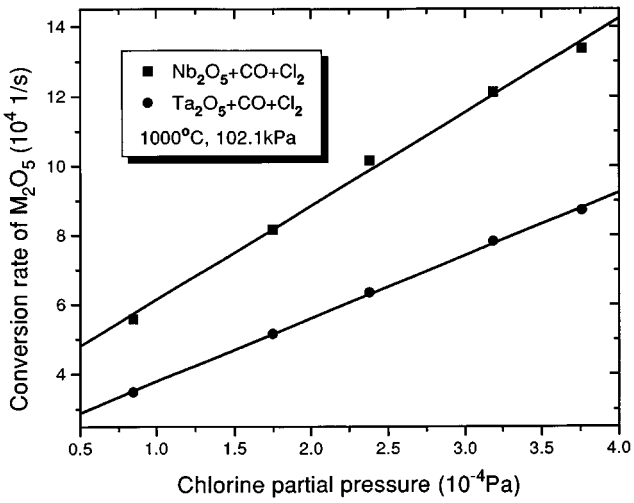

Figure 7. p_{Cl_2} vs. conversion rate of M_2O_5.

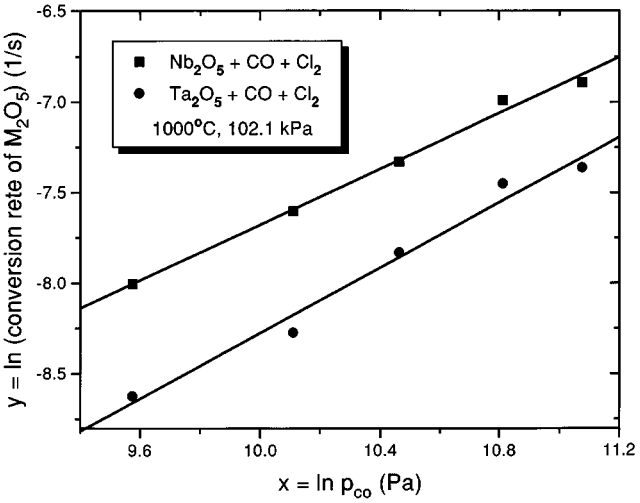

Figure 8. p_{CO} vs. conversion rate of M_2O_5.

It is important to estimate the correct average particle size in order to quantify the reactivity of the powder accurately enough. Obviously, the reactivity depends on the total surface area of the solid particle. Therefore, a good approximation can be achieved by assuming some idealized geometry (sphere in this study) and using the measured surface area to calculate an effective particle size, R_e (Rode and Hlavacek, 1995). This approach was also suggested by Szekely et al. (1976).

The BET surface area measurement by multipoint (5 points) analysis provided the following values for the oxide precursors: $S = 4.5972$ m^2/g for Ta_2O_5 and $S = 5.1596$ m^2/g for Nb_2O_5. For a single effective particle size and spherical geometry, the effective radius (R_e) can be expressed by the following relation:

$$R_e = \frac{3}{\rho^{\text{mass}}_{M_2O_5} S}. \tag{23}$$

The effective particle radius (R_e) calculated from Eq. 23 is 0.0796 μm for Ta_2O_5 and 0.1301 μm for Nb_2O_5.

Rate Constant and Other Kinetic Data. The reaction rate can be written as:

$$\text{For } Ta_2O_5: \qquad r = k_s p_{Cl_2} p_{CO}^{0.90}. \tag{24}$$

$$\text{For } Nb_2O_5: \qquad r = k_s p_{Cl_2} p_{CO}^{0.77}, \tag{25}$$

where

$$k_s = k_s^0 \exp\left(-\frac{E_a}{RT}\right). \tag{26}$$

By substituting the known values of $\tau_{800°C}$, $\tau_{1,000°C}$, $\rho_{M_2O_5}$, r_0 ($= R_e$), $p^m_{Cl_2}$, p^n_{CO} into Eq. 17, rate constants $k_{S,1,000°C}$ and $k_{S,800°C}$ can be calculated. The values of the activation energy, E_a, and the frequency factor k_s^0, can be determined from Eq. 26.

The calculation results are summarized in Table 1. It is obvious from the values of k_s or τ that the reactivity depends strongly on the reaction temperature.

$Ta_2O_5/Cl_2/C$ and $Nb_2O_5/Cl_2/C$ reaction systems

The thermodynamic analysis presented earlier indicates that in the temperature range $T = 800-1{,}000$°C, the major reaction product is the pentachloride, that

$$M_2O_5 + 5C + 5Cl_2 \rightarrow 2MCl_2 + 5CO.$$

Effect of Gas Flow Rate. Experiments were performed for M_2O_5:C = 3:1 (by weight) and Ar:Cl_2 = 2:1 (by volume) at 1,000°C for different values of the total flow rate. The reaction time was 5 min. The results obtained indicate that the limiting flow rate was 500 mL/min. Such values of the flow rate completely eliminate the effect of external diffusion in the packed-bed arrangement.

Effect of Chlorine Partial Pressure. Chlorination of M_2O_5:C = 3:1 (by weight) mixture was carried out at different Cl_2 partial pressures. The following reaction conditions were investigated: flow rate = 537 mL/min, temperature = 1,000°C, $P_{total} = 102.1$ kPa, and reaction time = 2 min. Argon was used to adjust the Cl_2 partial pressure and to keep the

Table 1. Kinetic Data of $Ta_2O_5 + CO + Cl_2$ and $Nb_2O_5 + CO + Cl_2$ Reaction Systems

Symbols	Descriptions	Unit	Ta_2O_5	Nb_2O_5
S	BET surface area of M_2O_5	cm^2/g	45,972	51,596
R_e ($= r_0$)	Effective (initial) particle radius of M_2O_5	cm	7.96×10^{-6}	1.30×10^{-5}
$\rho_{M_2O_5}$	Molar density of M_2O_5	mol/cm^3	0.0186	0.0168
m	Reaction order wrt Cl_2		1	1
n	Reaction order wrt CO		0.902	0.770
p_{Cl_2}	Partial pressure of Cl_2	Pa	37,595	37,595
p_{CO}	Partial pressure of CO	Pa	64,505	64,505
$\tau_{1,000°C}$	Time for complete conversion at 1,000°C	min	46.97	31.63
$\tau_{800°C}$	Time for complete conversion at 800°C	min	128.87	162.60
$k_{S,1,000°C}$	Rate constant at 1,000°C	mol/[cm$^2\cdot$min$\cdot$(Pa)$^{n+1}$]	3.86×10^{-18}	3.64×10^{-17}
$k_{S,800°C}$	Rate constant at 800°C	mol/[cm$^2\cdot$min$\cdot$(Pa)$^{n+1}$]	1.40×10^{-18}	7.08×10^{-18}
k_S^0	Frequency factor	mol/[cm$^2\cdot$min$\cdot$(Pa)$^{n+1}$]	8.93×10^{-16}	2.39×10^{-13}
E_a	Activation energy	J/mol	5.76×10^4	9.30×10^4

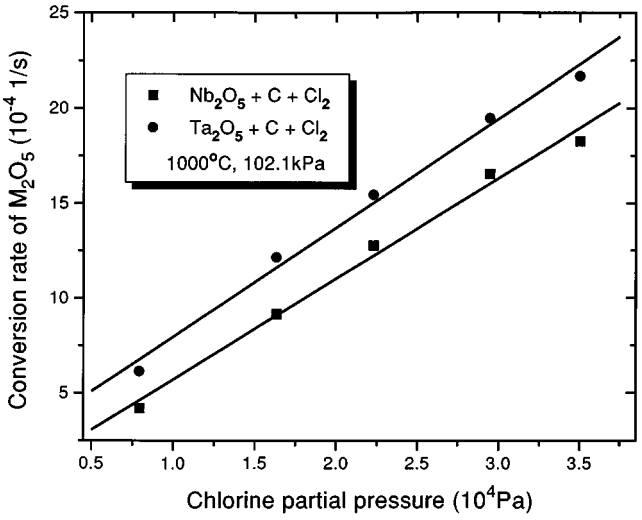

Figure 9. p_{Cl_2} vs. conversion rate of M_2O_5 (by $C+Cl_2$).

overall flow rate. A plot of ''conversion rate vs. Cl_2 partial pressure'' is shown in Figure 9. It is obvious that the relationship between reaction rate and partial chlorine pressure is linear for both systems.

Reaction Mechanism and Reaction Model. It can be inferred from the results of our experiments that at temperatures in the 800–1,000°C range, any binary reaction in the ternary component system (M_2O_5, carbon and chlorine) does not take place, or takes place only with extremely low conversion. Our thermodynamic calculations support this experimental observation. These facts lead to the following conclusions:

1. Formation of metal chloride by a direct reaction of Cl_2 with metal oxides does not take place, cf. Mellor (1945a).

2. Direct reduction of the oxides by carbon does not occur at the temperatures studied here. It is known that the reaction of tantalum or niobium oxides with carbon yields the corresponding carbides; however, the temperature must be higher than 1,600°C, cf. Ullmann (1985). Therefore, chlorination at these temperatures cannot be achieved via $M_2O_5 + C \rightarrow MC$ followed by $MC + Cl_2 \rightarrow MCl_5$.

3. The route of $C + Cl_2 \rightarrow CCl_4$ followed by $CCl_4 + M_2O_5 \rightarrow MCl_5$ also can be neglected, since carbon reacts with chlorine extremely slowly, cf. Mellor (1945b).

Solid–solid diffusion between carbon and oxide may occur, but since the diffusivity is of the order of magnitude of 10^{-10} to 10^{-15} cm^2/s, the diffusion process does not represent any significant mass flux and cannot be responsible for a relatively fast reaction rate.

Owing to the facts just listed, it is reasonable to assume that on the $M_2O_5/C/Cl_2$ interface, an activated $C/M_2O_5/Cl$ complex is formed at high temperatures. This active complex is very unstable and is instantaneously decomposed into CO and MCl_5. The formation rate of this active complex is the controlling step and is proportional to the surface area of the M_2O_5 particle, which is in contact with carbon and chlorine, that is, the kinetic behavior is controlled by phase boundary reactions (Tamhankar and Doraiswamy, 1979). Once this complex is formed it decomposes immediately. Therefore, the concentration of the complex is very low. Since C and Cl_2 are in excess, carbon is in the form of ultrafine particles, and Cl_2 is in the gaseous state, we suppose that the surface of a M_2O_5 particle is in good contact with C and Cl_2. Let W be the mass and A be the receding surface area of the remaining M_2O_5 particle. Consider a sphere of nonporous M_2O_5 of initial radius r_0, and density ρ, a rate equation then can be expressed as:

$$-\frac{dW}{dt} = kA \tag{27}$$

Here k is a rate constant and depends on temperature, carbon content, and chlorine partial pressure:

$$A = 4\pi r^2 \tag{28}$$

$$W = \rho \cdot \frac{4}{3}\pi r^3 \tag{29}$$

Differentiation of Eq. 29 with respect to time yields

$$\frac{dW}{dt} = 4\rho\pi r^2 \frac{dr}{dt} \tag{30}$$

The following equation can be obtained by simple derivation:

$$1-\left(1- X_{M_2O_5}\right)^{1/3} = \frac{k}{r_0\rho}t = Kt \tag{31}$$

Evidently, this equation is identical with Eq. 18, which was derived for the $M_2O_5/Cl_2/CO$ reaction systems.

Fitting of Experimental Data. Chlorination of the M_2O_5:C = 3:1 (by weight) mixture was carried out at 800°C and 1,000°C. To eliminate the mass-transfer resistance, a total flow rate of 537 mL/min was chosen, and argon was used as the diluting gas. Pressures in the system were kept at P_{total} = 102.1 kPa, $p_{Cl_2} = 35.0$ kPa, and $p_{Ar} = 67.1$ kPa. The plots of ''conversion vs. time'' are shown in Figures 10 and 11. The

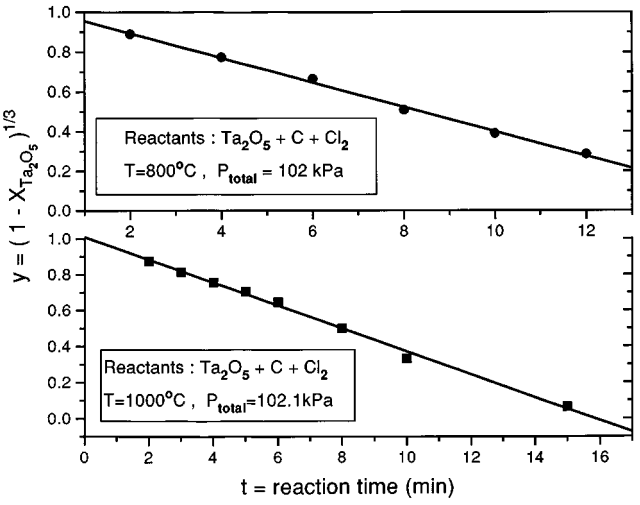

Figure 10. Conversion of Ta_2O_5 (by $C+Cl_2$) vs. time.

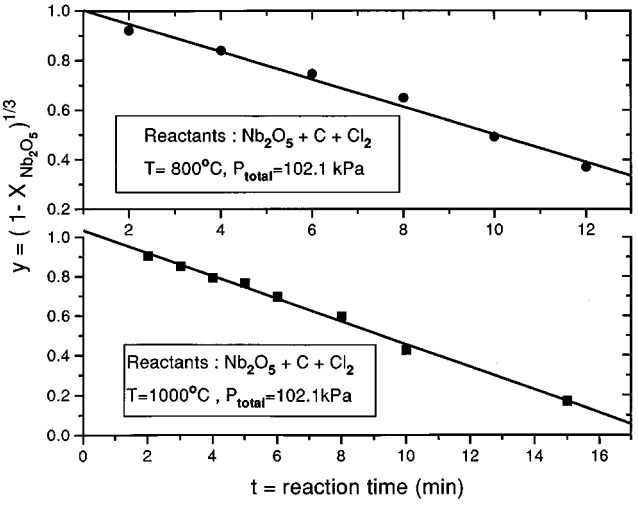

Figure 11. Conversion of Nb_2O_5 (by $C+Cl_2$) vs. time.

relation of "$(1-X_{M_2O_5})^{1/3}$ vs. time" is linear, as expected from Eq. 31. The values of K can be obtained and the values of rate constant k, can be calculated from the slopes of the plots.

Since k is a function of temperature, carbon content, and chlorine partial pressure, it can be expressed as

$$k = k_C \cdot k_{Cl_2} \cdot k_T. \tag{32}$$

Here k_C, k_{Cl_2}, and k_T represent the effect of carbon content, chlorine partial pressure, and reaction temperature, respectively.

Based on the linear relationship between reaction rate and chlorine partial pressure in Figure 9, we have $k_{Cl_2} = p_{Cl_2}$. We can also assume that with a sufficient amount of carbon, k_C is constant.

With

$$k_T = k_T^0 \exp\left(-\frac{E_a}{RT}\right),$$

Eq. 32 yields

$$k = p_{Cl_2} k_C k_T^0 \exp\left(\frac{-E_a}{RT}\right) \tag{33}$$

or

$$k = p_{Cl_2} k^0 \exp\left(\frac{-E_a}{RT}\right) \tag{34}$$

where $k^0 = k_C k_T^0$ is the frequency factor.

From the slopes of the curves drawn in Figures 10 and 11, the values of $K_{1,000°C}$ and $K_{800°C}$ can be obtained. Consequently, the values of $k_{1,000°C}$ and $k_{800°C}$ are calculated from Eq. 31. By substituting $k_{1,000°C}$, $k_{800°C}$, T, and p_{Cl_2} into Eq. 34, and assuming that E_a remains constant in the 800–1,000°C temperature range, the values of activation energy, E_a, and preexponential factor, k^0, can be calculated.

The results of calculations are summarized in Table 2.

Conclusions

Thermodynamic simulation and kinetic study reveal the following:

1. A complete conversion of M_2O_5 is feasible with Cl_2 as a chlorinating agent and either CO or C as the reducing agent.
2. Chlorination reactions of Ta_2O_5 and Nb_2O_5 have similar kinetic behavior. Reactions of the four systems in question are all first order with respect to Cl_2. Small differences in reaction order with respect to CO exist between $Ta_2O_5/Cl_2/CO$ and $Nb_2O_5/Cl_2/CO$.
3. Reactivity depends strongly on reaction temperature when using CO as the reducing agent; however, this effect is not so obvious with C.
4. MCl_5 is the major metal chloride generated for $M_2O_5/Cl_2/C$ systems in the 200 to 1,200°C temperature range, and for $M_2O_5/Cl_2/CO$ systems at temperatures from 200 to 1,000°C.
5. The reactivity is greatly enhanced by carbon. Reactivity in the CO system is lower. The activation energy in reacting systems with C is much lower than that with CO.
6. Experimental results and thermodynamic calculations established the existence of an activated $C/M_2O_5/Cl$ complex in $M_2O_5/Cl_2/C$ systems.
7. Experimental data can be represented by a shrinking-core model. Numerical values of rate equations were evaluated. These values can be used for purposes of scale-up.

Notation

K = constant, min^{-1}
m = reaction order with respect to Cl_2
n = reaction order with respect to CO

Table 2. Kinetic Data for $Ta_2O_5+C+Cl_2$ and $Nb_2O_5+C+Cl_2$ Reaction Systems

Symbols	Descriptions	Unit	Ta_2O_5	Nb_2O_5
$R_e\ (=r_o)$	Effective particle radius of M_2O_5 from BET	cm	7.96×10^{-6}	1.30×10^{-5}
$\rho^{mass}_{M_2O_5}$	Density of solid M_2O_5	g/cm^3	8.20	4.47
p_{Cl_2}	Partial pressure of Cl_2	Pa	34,994	34,994
$K_{1,000°C}$	Constant	min^{-1}	0.06379	0.05759
$K_{800°C}$	Constant	min^{-1}	0.06170	0.05569
$k_{1,000°C}$	Constant	g/(cm^2·min)	4.16×10^{-6}	3.35×10^{-6}
$k_{800°C}$	Constant	g/(cm^2·min)	4.03×10^{-6}	3.24×10^{-6}
k^0	Pseudofrequency factor	g/(cm^2·min·Pa)	1.41×10^{-10}	1.15×10^{-10}
E_a	Activation energy	J/mol	1,802.26	1,895.07

N_i = number of moles of species i, mol
p_i = partial pressure of species i, Pa
P_{total} = total pressure in the reaction system, Pa
r = radius of the unreacted part of solid particle at time t, cm
r_0 = initial radius of solid particle, cm
$V_{unreacted}$ = volume of unreacted core, cm^3
V_{total} = initial total volume of solid particle, cm^3
$\rho_{M_2O_5}$ or ρ = molar density of M_2O_5, moles/cm^3
$\rho^{mass}_{M_2O_5}$ = mass density of M_2O_5, g/cm^3

Literature Cited

Freitas, L., and F. Ajersch, ''Chlorination Kinetics of Nb_2O_5,'' *Chem. Eng. Commun.*, **30**, 19 (1984).

Johnstone, S. J., and M. G. Johnstone, *Minerals for the Chemical and Allied Industries*, 2nd ed., Wiley, New York, p. 414 (1961).

Levenspiel, O., *Chemical Reaction Engineering*, 2nd ed., Wiley, New York (1972).

McBride, B. J., and S. Gorden, *Computer Program for Calculation of Complex Chemical Equilibrium Compositions and Applications*, NASA Reference Publication 1311, NASA, Washington, DC (1996).

Mellor, J. W., ed., *Inorganic and Theoretical Chemistry*, Longmans, Green, London, Vol. IX, p. 897 (1945a), Vol. V, p. 822 (1945b).

Miller, G. L., ''The Separation of Tantalum and Niobium,'' *Ind. Chem.*, **35**(2), 175, **35**(3), 341, **35**(4), 443 (1959).

Rode, H., and V. Hlavacek, ''Detailed Kinetics of Titanium Nitride Synthesis,'' *AIChE J.*, **41**, 377 (1995).

Szekely, J., et al., *Gas-Solid Reactions*, Academic, New York (1976).

Tamhankar, S. S., and L. K. Doraiswamy, ''Analysis of Solid-Solid Reactions: A Review,'' *AIChE J.*, **25**, 561 (1979).

Ullmann's Encyclopedia of Industrial Chemistry, 5th ed., Vol. A5, Verlag Chemie, Weinheim, p. 69, 70 (1985).

Yang, F., and V. Hlavacek, ''Carbochlorination of Oxides of Transition Group Metals,'' AIChE Meeting, Los Angeles, CA (1997).

Yang, F., and V. Hlavacek, ''Carbochlorination Kinetics of Titanium Dioxide with Carbon and Carbon Monoxide as Reductant,'' *Met. Mater. Trans.*, **29B**, 1297 (1998).

Manuscript received June 23, 1998, and revision received Jan. 12, 1999.